



## SPECTRAL CHARACTERIZATION OF SELF-ASSOCIATION OF ANTITUMOR DRUG MITOXANTRONE

Mirela ENACHE<sup>a</sup> and Elena VOLANSCHI<sup>b\*</sup>

<sup>a</sup>"I. Murgulescu" Institute of Physical Chemistry, Roumanian Academy, Splaiul Independentei 202, Bucharest 060021, Roumania

<sup>b</sup>Department of Physical Chemistry, Faculty of Chemistry, University of Bucharest, Blvd. Elisabeta 4-12, Bucharest 030018, Roumania

Received July 29, 2009

Self-association of antitumor drug mitoxantrone, a process that is known to compete *in vitro* with the binding of the drug to DNA was studied by absorption spectroscopy in aqueous and micellar solutions, at different pH values. The variation of the molar absorption coefficient of mitoxantrone with increasing concentration was observed at the pH values investigated, and these results were interpreted in terms of a dimerization model. The results indicate that in aqueous solutions mitoxantrone forms dimers at concentrations higher than  $1 \times 10^{-6}$  M, and the process is dependent on pH, the dimerization constant increasing with the increase of pH. The presence of SDS and CTAB surfactants at concentrations above their CMC induces the dissociation of mitoxantrone aggregates with encapsulation of the monomers into the surfactant micelles.

### INTRODUCTION

Mitoxantrone is a synthetic anthracenedione antitumor drug which was developed based on the anthracycline structure, in an attempt to find anthracycline analogues with decreased cardiotoxicity but with the same antitumor efficacy.<sup>1</sup> However, unlike anthracyclines, mitoxantrone is not active against a wide spectrum of tumors, being used specifically for the treatment of advanced breast cancer, non-Hodgkins lymphoma, non-lymphocytic leukemia and melanoma.<sup>2</sup> If early reports indicate that mitoxantrone has a lower risk of cardiac side effects compared with anthracyclines,<sup>3</sup> this conclusion has been changed in more recent studies, which indicate that mitoxantrone causes chronic cardiotoxicity.<sup>4,5</sup> Also, its clinical usefulness is limited by the occurrence of multidrug resistance (MDR) associated with the overexpression of membrane transporters.<sup>6</sup> Different mechanisms have been proposed for mitoxantrone antitumour effects including DNA intercalation,<sup>7</sup> inhibition of topoisomerase II<sup>8</sup> and DNA crosslinking after its metabolic activation by cellular oxidoreductases.<sup>9,10</sup>

The efficacy of cancer chemotherapy can be improved by the encapsulation of the drugs in carrier systems, in order to ensure the transport to specific sites of action without loss and also with minimal interaction with healthy cells.<sup>11</sup> In this context, the micellar systems (colloidal-sized clusters formed by surfactants in solutions) can be used as drug carriers in numerous drug delivery and drug targeting systems.<sup>12,13</sup>

The structure of mitoxantrone is shown in Fig. 1. Mitoxantrone has a planar heterocyclic ring substituted with two positively charged nitrogen-containing side chains.

The dose of antitumor drugs used clinically is generally more than tens of micromolar concentration.<sup>14</sup> At these concentrations, self-association was shown occur in aqueous solutions and compete with DNA binding.<sup>15-17</sup> Therefore, prior to determine the structural and thermodynamical characteristics of the binding of these drugs to DNA, it is necessary to analyze the self-association of drugs in solution. The self-association of these drugs also plays a biological role, affecting their transport across bilayer lipid membrane and consequently influencing the antitumor action.<sup>18,19</sup>

\* Corresponding author: [elenavolanschi@gmail.com](mailto:elenavolanschi@gmail.com)

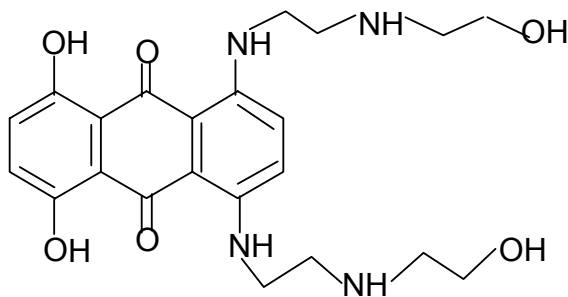


Fig. 1 – Chemical formula of mitoxantrone.

The aim of the present paper is to investigate the aggregation of mitoxantrone in aqueous solution and the influence of different factors, like pH and the presence of anionic (sodium dodecyl sulfate, SDS) and cationic (cetyltrimethyl ammonium bromide, CTAB) surfactants micelles.

## MATERIALS AND METHODS

Mitoxantrone and the surfactants, SDS and CTAB were purchased from Sigma and used without further purification. Drug solutions were prepared in Hydrion Buffer (phosphate buffer pH 7.4 and 5; carbonate buffer pH 10) from Sigma, and the measurements were carried out at room temperature. Mitoxantrone concentrations were determined spectrophotometrically at the isosbestic point between monomer/dimer transitions at 682 nm, using the molar absorption coefficient  $\epsilon = 8360 \text{ M}^{-1} \text{ cm}^{-1}$ .<sup>17</sup> Absorption spectra were measured with a Unicam-UV 4 Helios spectrophotometer. The decomposition of absorption spectra was performed using Peak Fit 4.11 software.

## RESULTS AND DISCUSSION

### 1. Dimerization in aqueous solutions

The absorption spectra of mitoxantrone in phosphate buffer pH 7.4 at different concentrations are presented in Fig. 2a and, it can be observed that the shape of the spectrum is dependent on concentration. This dependence is usually assigned to the formation of molecular aggregates, by analogy with other cationic dyes and drugs.<sup>20-23</sup> Also, at very low concentrations (up to  $6.58 \times 10^{-6} \text{ M}$ ) the intensity of both absorbance maxima is similar, but, with increasing concentration, the

band at 610 nm becomes more intense than that at 660 nm. The decomposition of the absorption spectra in elementary bands for spectra 1 and 5 in Fig. 2a is presented in Fig. 2b, c.

By comparison with literature data on other dyes and drugs,<sup>20-23</sup> the band at 660 nm was assigned to the monomer (M) and the band at 610 nm to the dimer (D). The band around 560 nm, which increases in intensity at concentrations higher than  $10^{-4} \text{ M}$ , was assigned to the formation of aggregates beyond dimers, i.e. trimers.

The increase of drug concentration leads to a decrease in the intensity of absorbance maxima at 660 nm while the intensity of absorbance maxima at 610 nm increases. As the contribution of multimers is low, the aggregation process may be modeled in terms of a simple dimerization process that can be followed by measuring the ratio of absorbances ( $A_M/A_D$ ) at absorption maxima of mitoxantrone corresponding to monomer (660 nm) and dimer (610 nm). Evolution of this ratio for spectra 1-5, presented as insert in Fig. 2a, shows a constant decrease with drug concentration. Regarding the evolution of the absorbance at 560 nm, assigned to the formation of aggregates beyond dimers, i.e. trimers, it may be stated that for the drug concentrations corresponding to the spectra 1 – 5, the calculated contribution of the trimers considering also the trimerization equilibrium ( $D + M \rightarrow T$ ) is in the range 4 – 10%, showing that at concentrations of mitoxantrone in the range  $10^{-6} - 10^{-5} \text{ M}$  used in this study, the predominant species in the solution are the monomer and the dimer. Our results are in agreement with literature data,<sup>24</sup> which have reported that even for higher drug concentration ( $5 \times 10^{-4} \text{ M}$ ), the contribution of trimers and higher aggregates is reduced.

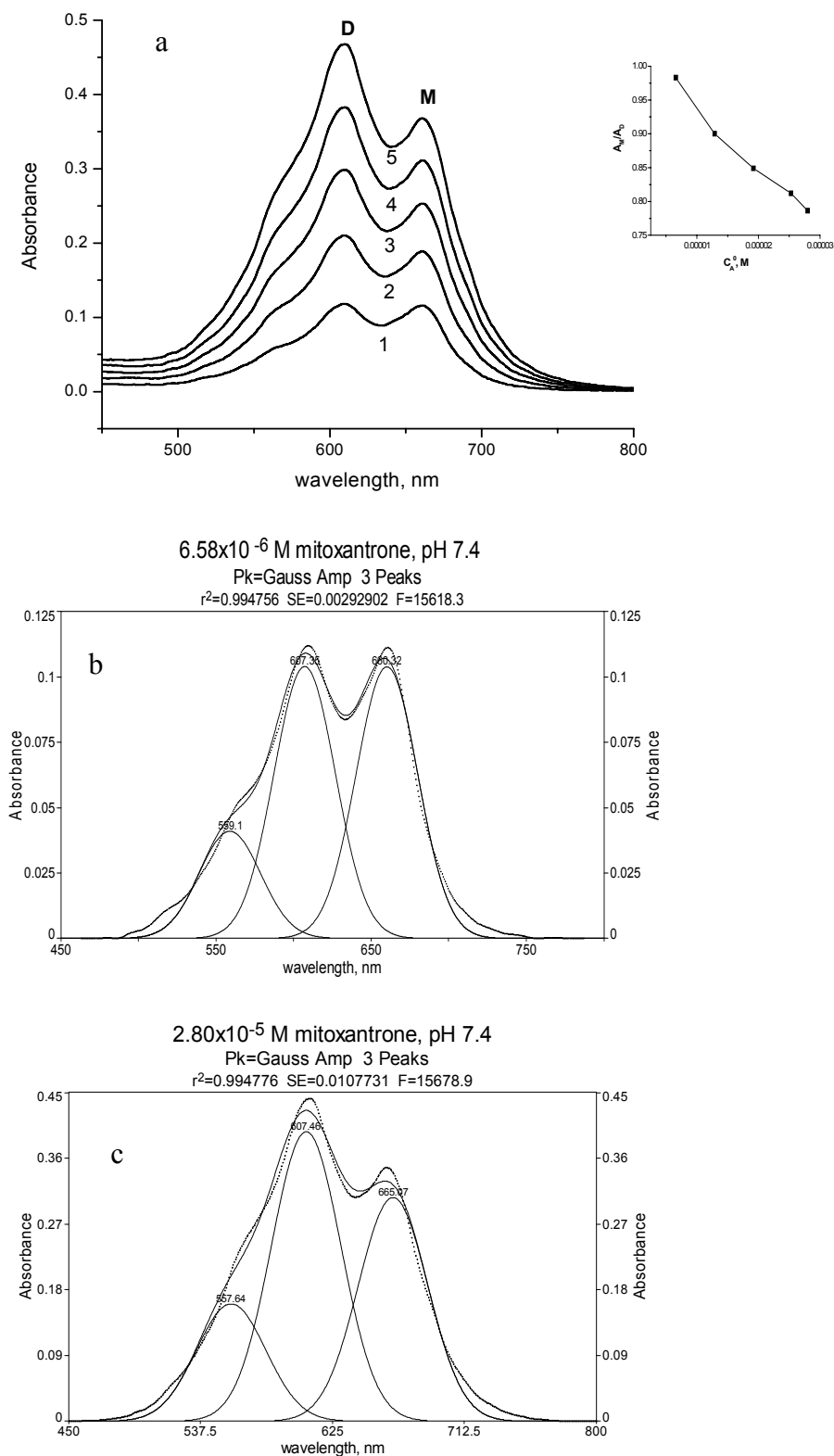


Fig. 2 – a) Absorption spectra of mitoxantrone in phosphate buffer pH 7.4, as a function of concentration: 1 –  $6.58 \times 10^{-6}$  M, 2 –  $1.29 \times 10^{-5}$  M, 3 –  $1.92 \times 10^{-5}$  M, 4 –  $2.53 \times 10^{-5}$  M, 5 –  $2.80 \times 10^{-5}$  M; inset – the variation of  $A_M/A_D$  ratio in function of mitoxantrone concentration. b), c) Decomposition of the absorption spectra 1 and 5 from the family of spectra in Fig. 2a.

The dimerization constant at pH constant and the molar absorption coefficient of the dimer were calculated by methods described by Schwarz<sup>25</sup> and Tipping,<sup>26</sup> considering only the monomer - dimer equilibrium, for three pH values: 7.4, 5 and 10:

$$2M \rightleftharpoons D \quad nH \quad K_d \quad \frac{C_D C_H^n}{C_M^2} \quad K'_d C_H^n \quad (1)$$

where M – monomer, D – dimer,  $K_d$  – dimerization constant,  $C_D$ ,  $C_M$  – concentrations of the monomer and dimer, respectively. The dimerization constant at constant pH value,  $K'_d$ , was determined from the dependence of the absorbance in function of drug concentration, at different pH values.

Starting from the dimerization equilibrium, the total absorbance is given by:

$$A = \epsilon_{app} C_A^0 l = (\epsilon_M C_M + 2\epsilon_D C_D) l \quad (2)$$

where  $\epsilon_{app}$ ,  $\epsilon_M$  and  $\epsilon_D$  denote the absorption coefficients at 660 nm of the solution, the pure monomer and the pure dimer, respectively and  $C_A^0$  is the total drug concentration, and  $l = 1$  cm.

Mass conservation requires:

$$C_A^0 = C_M + 2C_D \quad (3)$$

For very low drug concentrations ( $\sim 10^{-6}$  M),  $C_M \gg C_D$ , and, at the limit,  $\epsilon_{app} = \epsilon_M$ . For higher concentrations ( $\sim 10^{-4}$  M), the reverse is true,  $C_M \ll C_D$ , and  $\epsilon_{app} = \epsilon_D$ .

The plot of the apparent molar absorption coefficient in function of the total concentration of mitoxantrone in the range  $10^{-6}$  M –  $10^{-4}$  M is presented in Fig. 3. Sigmoidal fit of the curve allows to determine the dimerization constant,  $K'_d = 1.05 \times 10^5 \text{ M}^{-1}$  at pH 7.4 and the molar absorption coefficient of dimer,  $\epsilon_D = 7889 \text{ M}^{-1} \text{ cm}^{-1}$ .

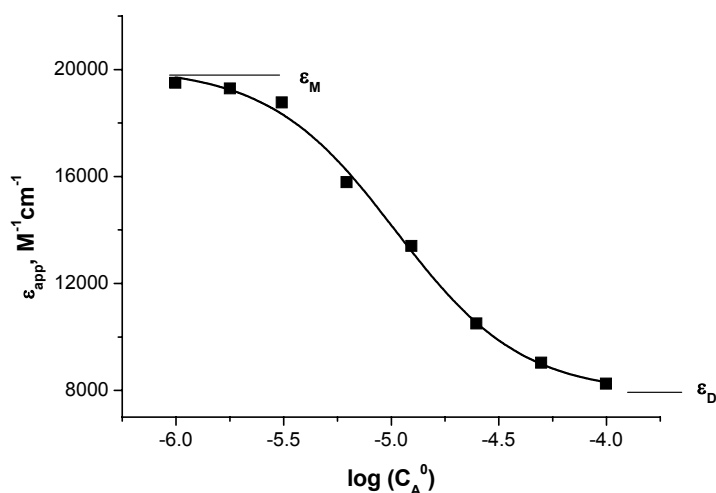


Fig. 3 – Concentration dependence of the apparent molar absorption coefficient  $\epsilon_{app}$  of mitoxantrone at  $\lambda = 660$  nm, in phosphate buffer pH 7.4.

By combining equations (1), (2) and (3),  $C_M$  and  $C_D$  can be eliminated and the result can be represented as:

$$\sqrt{\frac{\epsilon_M - \epsilon_{app}}{C_A^0}} = \sqrt{\frac{2K'_d}{\Delta\epsilon} [\Delta\epsilon - (\epsilon_M - \epsilon_{app})]} \quad (4)$$

where  $\Delta\epsilon = \epsilon_M - \epsilon_D$ . Accordingly a plot of  $\sqrt{(\epsilon_M - \epsilon_{app})/C_A^0}$  versus  $(\epsilon_M - \epsilon_{app})$  should yield a straight line with the intercepts  $\sqrt{2K'_d \Delta\epsilon}$  (on the

ordinate axis) and  $\Delta\epsilon$  (on the abscissa axis) (Fig. 4a).

Alternative treatment of the dimerization equilibrium was performed using the method described by Tipping<sup>26</sup> that utilizes the equation:

$$\sqrt{\frac{C_A^0}{\epsilon_M - \epsilon_{app}}} = \frac{1}{\epsilon_M - \epsilon_D} \sqrt{C_A^0 (\epsilon_M - \epsilon_D)} + \sqrt{\frac{1}{2K'_d (\epsilon_M - \epsilon_D)}} \quad (5)$$

The plot corresponding to equation (5) is presented in Fig. 4b and the results are presented in Table 1.

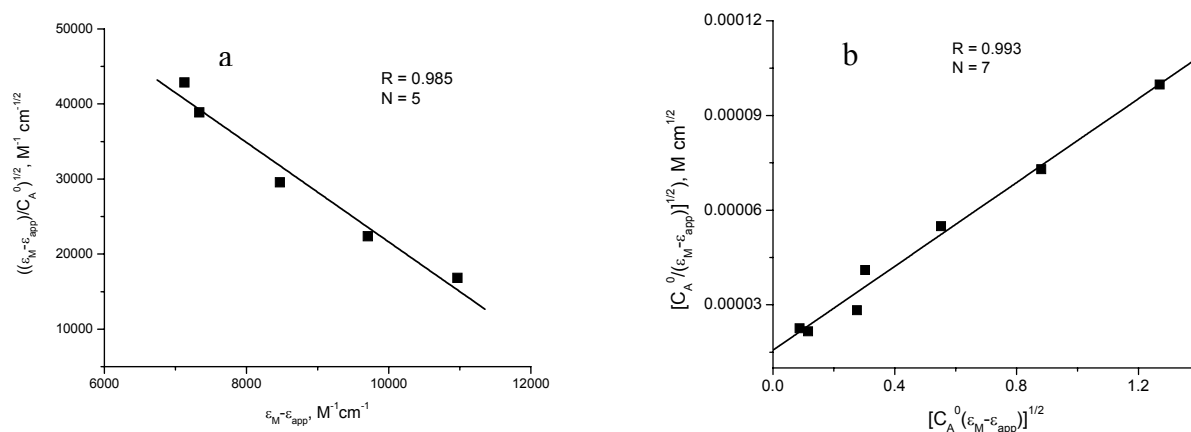


Fig. 4 – Plots to determine the dimerization constant and molar absorption coefficient of the dimer for mitoxantrone: a) according to equation (4), at pH 10 and b) according to equation (5), at pH 7.4.

Table 1

Dimerization constant at constant pH ( $K_d$ ), the absorption molar coefficient of dimer ( $\epsilon_D$ ) and spectral parameters of mitoxantrone ( $2.80 \times 10^{-5}$  M) at pH 5, 7.4 and 10.

	pH 5	pH 7.4	pH 10
$K_d$ , $M^{-1}$	$(2.44 \pm 0.18) \times 10^4$	$(0.75 \pm 0.37) \times 10^5$	$(2.76 \pm 0.21) \times 10^5$
$\epsilon_D$ , $M^{-1}cm^{-1}$	$14427 \pm 190$	$7750 \pm 550$	$608 \pm 181$
$\lambda_D$ , nm	611	610	614
$\lambda_M$ , nm	663	660	666
$A_M/A_D$	1.07	0.79	0.68

The results in Table 1 outline that the dimerization constant at pH 7.4  $K_d$  ( $0.75 \times 10^5 M^{-1}$ ) and molar absorption coefficient of the dimer,  $\epsilon_D$  ( $7750 M^{-1}cm^{-1}$ ) are in good agreement with the values obtained from the sigmoidal plot in Fig. 3, indicating that the dimerization process of the drug is associated with a decrease of the apparent molar absorption coefficient

from the value corresponding to the monomer ( $19500 M^{-1}cm^{-1}$ ) to the dimer value.

The influence of pH on the dimerization equilibrium is outlined by the spectra in Fig. 5 and the data in Table 1. The spectra in Fig. 5 show the decrease of the intensity of the monomer band with increasing pH, with an isobestic point at 688 nm.

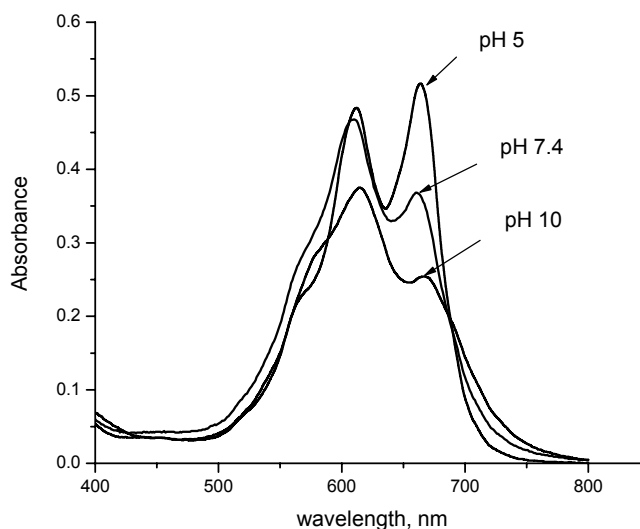


Fig. 5 – Absorption spectra of mitoxantrone ( $2.80 \times 10^{-5}$  M) at different pH values.

At pH 10, the absorbance maxima are red shifted and the  $A_M/A_D$  ratio (Table 1) decreases from 0.79 for mitoxantrone ( $2.80 \times 10^{-5}$  M) in phosphate buffer pH 7.4 at 0.68, indicating that dimerization process is favored in basic environment. The dimerization was found to be reversible and should be related to the deprotonation of  $\text{NH}_3^+$  groups of the side-chains at basic pH.<sup>27</sup> At pH 5, the position of the absorbance maxima are less affected and the  $A_M/A_D$  ratio increases from 0.79 in phosphate buffer pH 7.4 at 1.07, suggesting the dissociation of the drug dimers (Table 1).

It can be observed that with the increase of pH, the dimerization constant increases and the molar absorption coefficient of the dimer decreases.

## 2. Influence of surfactant on the dimerization process

The importance of micellar systems in the pharmaceutical field as possible drug delivery systems has been already outlined.<sup>12,13</sup> Therefore, the dimerization process of mitoxantrone has also been investigated in the presence of anionic (sodium dodecyl sulfate, SDS) and cationic (cetyltrimethyl ammonium bromide, CTAB) surfactant micelles. The plot of the apparent molar absorption coefficient at 660 nm ( $\epsilon_{\text{app}}$ ) in function of SDS to drug concentration ratio (P/D) in Fig. 6a outlines two distinct processes, depending on the surfactant concentration: Process I in the pre-micellar range was assigned to the interaction of the drug with surfactant molecules, which

reduces the repulsion between positively charged drug molecules and favors the dimerization of the drug. The decrease of  $\epsilon_{\text{app}}$  from the value characteristic for the monomer to  $8328 \text{ M}^{-1}\text{cm}^{-1}$  close to the  $\epsilon_D$  value at pH 7.4 in Table 1, is strong support for the dimerization process induced by the surfactant in the pre-micellar concentration range. Process II at surfactant concentration higher than CMC, corresponds to the encapsulation of the drug into micelles, predominantly in monomeric form. Similar behavior was observed for other antitumor drugs, actinomycin D and doxorubicin.<sup>28,29</sup>

The absorption spectra of mitoxantrone ( $3.55 \times 10^{-5}$  M) in phosphate buffer pH 7.4, in presence of micellar concentrations of SDS and CTAB are presented in Fig. 6b and the spectral parameters of mitoxantrone in the presence of both surfactants at two pH values are collected in Table 2. Analysis of spectra in Fig. 6b shows that at similar mitoxantrone concentrations ( $\sim 3 \times 10^{-5}$  M), the  $A_M/A_D$  ratio increases from 0.79 in the absence of surfactants (Table 1) to 1.26 in the presence of anionic surfactant, SDS, and 0.85 in the presence of cationic surfactant, CTAB. Moreover, the spectrum in micellar concentration of SDS is quite similar to the spectrum in DMSO,<sup>30</sup> which may be considered further support for the hydrophobic environment of drug molecules, attesting for the encapsulation of the drug in SDS micelles as monomer. The smaller effect of the cationic surfactant CTAB may be explained by the electrostatic repulsion between the positive drug charges and cationic surfactant CTAB.

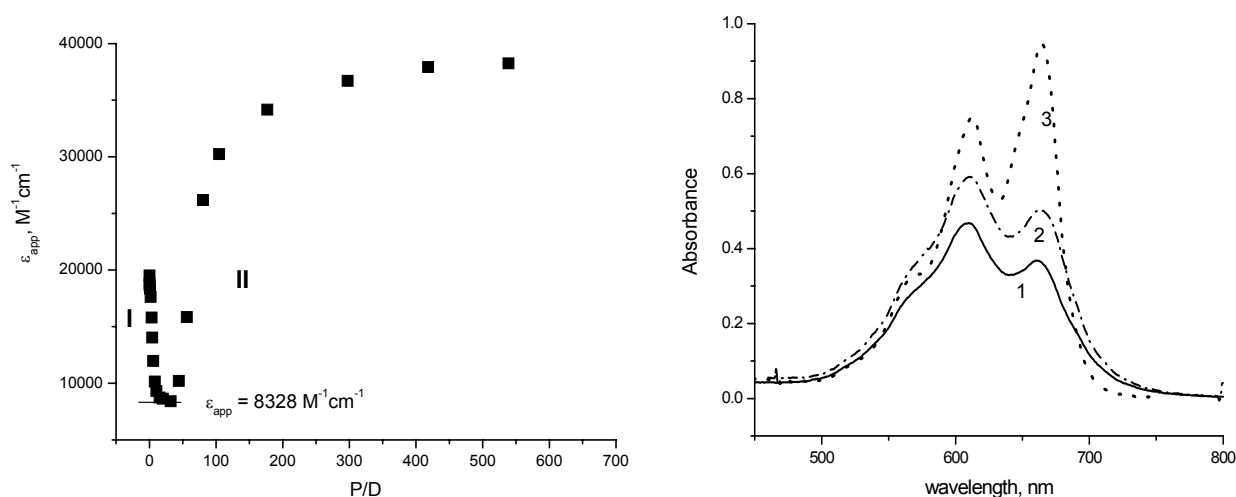


Fig. 6 – a) Dependence of the apparent molar absorption coefficient at 660 nm ( $\epsilon_{\text{app}}$ ) on SDS / drug ratio (P/D): process I –  $C_{\text{SDS}} < \text{CMC}$ , and process II –  $C_{\text{SDS}} > \text{CMC}$ . b) Absorption spectra of mitoxantrone ( $3.55 \times 10^{-5}$  M) in phosphate buffer pH 7.4 in the absence of surfactant (spectrum 1 – full line) and in the presence of micellar concentrations of SDS ( $3.19 \times 10^{-3}$  M, spectrum 3 – dash line) and CTAB ( $8.52 \times 10^{-4}$  M, spectrum 2 – dash dot line).

Table 2

Spectral parameters of mitoxantrone ( $3.55 \times 10^{-5}$  M) in the presence of surfactant micelles

	SDS ( $3.19 \times 10^{-3}$ M)		CTAB ( $1.65 \times 10^{-3}$ M)	
	pH 7.4	pH 10	pH 7.4	pH 10
$\lambda_D$ , nm	613	618	610	623
$\lambda_M$ , nm	664	672	663	677
$A_M/A_D$	1.26	1.20	0.85	1.40

As it can be seen in Fig. 6 and in Table 2, the absorption maxima of monomer and dimer in the presence of SDS and CTAB concentrations above their CMC ( $1.99 \times 10^{-3}$  M for SDS<sup>31</sup> and  $5.7 \times 10^{-5}$  M for CTAB<sup>32</sup>) are slightly red shifted as compared to the drug spectrum in buffer solutions in Table 2 at the corresponding pH values.

Also, the  $A_M/A_D$  ratio increases in the presence of surfactants micelles as against the values in the absence of surfactant in Table 1, suggesting the dissociation of the drug dimers. At physiological pH, the highest value of  $A_M/A_D$  ratio is noted for SDS micelles, indicating that the anionic surfactant micelles induce a higher dissociation of mitoxantrone dimers in comparison with cationic surfactant, CTAB. At pH 7.4 mitoxantrone molecule has two positively charged nitrogen-containing side chains so that it is expected to have strong electrostatic interactions with anionic surfactant, SDS. At SDS concentrations higher than CMC, surfactant micelles are formed and the drug is encapsulated in micelles in monomer form.

## CONCLUSIONS

Our investigation showed that mitoxantrone forms dimers in aqueous solution at concentrations higher than  $1 \times 10^{-6}$  M, and the value of the dimerization constant at physiologically pH indicates that the concentration of mitoxantrone in monomer form drastically decreases from ~87% at a total drug concentration of  $1 \times 10^{-6}$  M to ~23% at a total drug concentration of  $1 \times 10^{-4}$  M. Results indicate also that the dimerization process is dependent on pH, the dimerization constant increasing with the increase of pH. Regarding the influence of different surfactant micelles, our results outline that the presence of an anionic surfactant (SDS) at concentrations above their CMC induces the dissociation of the mitoxantrone dimers, in greater extent than cationic surfactant (CTAB). Therefore, in delivery formulations based on surfactants at doses of antitumor drugs higher than tens of micromolar concentration, as are used clinically<sup>14</sup>, the dimer amount is reduced, which

may increase the efficiency of drug transport to tumors and influence the antitumor action.

*Acknowledgements:* The financial support of the Roumanian Ministry of Education and Research through CNCIS Grant IDEI no. 486/2009 is gratefully acknowledged.

## REFERENCES

1. G. Minotti, P. Menna, E. Salvatorelli, G. Cairo and L. Gianni, *Pharmacol. Rev.*, **2004**, *56*, 185-229.
2. M.A. Cornbleet, R.C. Stuart-Harris, I.E. Smith, R.E. Coleman, R.D. Rubens, M. McDonald, H.T. Mouridsen, H. Rainer, A.T. Van Oosterom and J.F. Smyth, *Eur. J. Cancer Oncol.*, **1984**, *20*, 1141-1146.
3. M. Estorch, I. Carrio, D. Martinez-Duncker, L. Berna, G. Torres, C. Alonso and B. Ojeda, *J. Clin. Oncol.*, **1993**, *11*, 1264-1268.
4. X. Thomas, Q.H. Le and D. Fiere, *Ann. Hematol.*, **2002**, *81*, 504-507.
5. R.E. Gonsette, *J. Neurol. Sci.*, **2003**, *206*, 203-208.
6. C. Nieth and H. Lage, *J. Chemother.*, **2005**, *17*, 215-223.
7. P.J. Smith, S.A. Morgan, M.E. Fox and J.V. Watson, *Biochem. Pharmacol.*, **1990**, *40*, 2069-2078.
8. M.P. Boland, K.A. Fitzgerald and L.A.J. O'Neill, *J. Biol. Chem.*, **2000**, *275*, 25231-25238.
9. K. Mewes, J. Blanz, G. Ehninger, R. Gebhardt and K.P. Zeller, *Cancer Res.*, **1993**, *53*, 5135-5142.
10. A. Skladanowski and J. Konopa, *Br J. Cancer*, **2000**, *82*, 1300-1304.
11. C.O. Rangel-Yagui, A. Pessoa-Jr and L. C. Tavares, *J. Pharm. Pharmaceut. Sci.*, **2005**, *8*, 147-163.
12. M.C. Jones and J.C. Leroux, *Eur. J. Pharm. Biopharm.*, **1999**, *48*, 101-111.
13. M.E. Dalmora, S.L. Dalmora and A.G. Oliveira, *Int. J. Pharm.*, **2001**, *222*, 45-55.
14. P. Agrawal, S.K. Barthwal and R. Barthwal, *Eur. J. Med. Chem.*, **2009**, *44*, 1437-1451.
15. J.B. Chaires, N. Dattagupta and D.M. Crothers, *Biochemistry*, **1982**, *21*, 3927-3932.
16. T. Oncescu, I. Iliescu and L. De Mayer, *Biophys. Chem.*, **1993**, *47*, 277-283.
17. J. Kapuscinski and Z. Darzynkiewicz, *Biochem. Pharmacol.*, **1985**, *34*, 4203-4213.
18. D.B. Davies, D.A. Veselkov, M.P. Evstigneev and A.N. Veselkov, *J. Chem. Soc., Perkin Trans.*, **2001**, *2* 61-67.
19. M.P. Evstigneev, V.V. Khomich and D.B. Davies, *Russ. J. Phys. Chem.*, **2006**, *80*, 741-746.
20. R.E. Ballard and C.H. Park, *J. Am. Chem. Soc.*, **1970**, *92*, 1340-1343.
21. E. Volanschi and L.-E. Vajan, *Rev. Roum. Chim.*, **2001**, *46*, 163-173.

22. D.B. Davies, L.N. Djimant and A.N. Veselkov, *J. Chem. Soc. Faraday Trans.*, **1996**, *92*, 383-390.
23. M. Enache, M. Hilebrand and E. Volanschi, *Romanian J. Biophys.*, **2001**, *11*, 93-105.
24. B.S. Lee and P.K. Dutta, *J. Phys. Chem.*, **1989**, *93*, 5665-5672.
25. G. Schwarz, *Eur. J. Biochem.*, **1970**, *12*, 442-453.
26. E. Tipping, B. Ketterer and P. Poskelo, *Biochem. J.*, **1978**, *169*, 509-516.
27. A. Feofanov, S. Sharonov, I. Kudelina, F. Fleury and I. Nabiev, *Biophys. J.*, **1997**, *73*, 3317-3327.
28. M. Enache, I. Serbanescu, D. Bulcu and E. Volanschi, *Rev. Roum. Chim.*, **2007**, *52*, 725-731.
29. M. Enache, D. Bulcu and E. Volanschi, *J. Colloid Surface Chemistry*, **2008**, *8*, 43-51.
30. M. Enache, C. Bendic and E. Volanschi, *Bioelectrochemistry*, **2008**, *72*, 10-20.
31. E. Fuguet, C. Rafols, M. Roses and E. Bosch, *Anal. Chim. Acta*, **2005**, *548*, 95-100.
32. N. Chidambaram and D.J. Burgess, *Colloids Surfaces A: Physicochem. Eng. Aspects*, **2001**, *181*, 271-275.